DOI: 10.17344/acsi.2022.7350 *Acta Chim. Slov.* **2022,** *69,* 458–465

Scientific paper

Adsorption Properties of Low-Cost Synthesized Nanozeolite L for Efficient Removal of Toxic Methylene Blue Dye from Aqueous Solution

Neda Salek Gilani,[1,*] Salma Ehsani Tilami[2] and Seyed Naser Azizi[1]

[1] *Analytical division, Faculty of Chemistry, University of Mazandaran, Postal code 47416-95447, Babolsar, Iran*

[2] *Department of basic science, Farhangian University, Postal code 19989-63341, Tehran, Iran*

[*] *Corresponding author: E-mail: salekgilani@gmail.com*

Received: 01-07-2022

Abstract

In this study, nanozeolite L was applied for the removal of toxic methylene blue dye (MB) to evaluate its feasibility as an effective adsorbent. Synthesized nanozeolite L was characterized by Xray diffraction (XRD), Fourier transform infrared (FTIR), scanning electronic microscopy (SEM), Brunauer–Emmett–Teller (BET), and energy-dispersive Xray analysis (EDX) methods to determine its basic physicochemical properties. Batch adsorption studies were performed as a function of pH, adsorbent dose, contact time, initial MB concentration, and temperature. The adsorption behavior of MB was fitted better by the Langmuir isotherm than by the Freundlich isotherm, and the maximum adsorption capacity of nanozeolite L was obtained 80.64 mg g^{-1}. The negative values of Gibbs free energy change ($\Delta G°$) and the positive value of the standard enthalpy change ($\Delta H°$) affirmed that the adsorption process is spontaneous and endothermic. Based on these findings, nanozeolite L, with high surface area, great adsorption capacity, and low synthetic cost, can be an effective and economical adsorbent for MB removal.

Keywords: Nanozeolite L; Hydrothermal synthesis; Methylene blue; Adsorption

1. Introduction

The discharge of dye effluents from various industries such as paper, textiles, leather, plastics, rubber, cosmetics, and food beverages to the environment, especially to the water system, is becoming a major concern because of their toxicity. The considerable release of dyes from these industries is a major problem of pollution, leading to severe damages to aquatic life. Dyes can consume the dissolved oxygen necessary for aquatic life, and also some of them have direct toxicity to microbial populations and even can be toxic and carcinogenic to mammals.[1–3]

Methylene blue (MB) is a cationic aromatic dye and has several adverse effects on Homo sapiens, such as an increase in hypertension, nausea, diarrhea, headache, dizziness, and eye injuries. So it must be removed from wastewater before discharge into water bodies.[4–6]

Various physical and chemical methods such as coagulation, sedimentation, ozonation, membrane separation, photocatalysis, and adsorption have been used for the removal of dyes from wastewaters.[7,8] Among these methods, the adsorption process is preferred because of its high efficiency and cost-effectiveness.[9,10] The selection of adsorbent plays a significant role in determining its cost-effectiveness, and the search for efficient and low-cost adsorbents such as natural, agricultural, and industrial byproduct waste is still underway.[11–13] Clay materials such as bentonite, montmorillonite, kaolinite, and zeolite have received much attention due to their unique structural and surface features, which offer high chemical stability and specific surface area that conduces to high adsorption capacities.[14-22] Among these clays, zeolite has received the greatest consideration and recognition as an appropriate adsorbent.

Among a large number of zeolites, zeolite L is one of the most interesting and versatile adsorbents. It contains one-dimensional (1D) channels running along the length of its hexagonal crystals. The unique configuration of its large pores with a diameter of 7.1 Å makes this kind of zeolite an excellent candidate for shape-selective catalysis, for the adsorption of various species such as ions, metals, and organic molecules and mass transport and/or occlu-

sion.[23,24] The reduction of zeolite size from the micrometer to the nanometer scale leads to unique properties such as decreased diffused path lengths and large external surfaces, which are effective for improving the adsorption of organic dye pollutants.[25,26] Most nanozeolites are synthesized in the presence of costly organic structure-directing agents (OSDAs), but nanozeolite L could be synthesized in the absence of OSDAs, which is desirable due to economic considerations.[27]

The main objective of the present study is to evaluate the feasibility of using synthesized nanozeolite L as a cost-effective adsorbent for removing MB from aqueous solution. The effects of various adsorption parameters such as solution pH, adsorbent dose, reaction time, initial pollutant concentration, and temperature on adsorption of MB were investigated. Also, the adsorption isotherm, kinetic, and thermodynamic were studied. This fundamental study would be useful for further application in designing a batch reactor for the treatment of dye-containing wastewaters coming out from various industries.

2. Experimental

2. 1. Chemicals and Apparatus

Silicic acid, potassium hydroxide (≥ 85.0 %), and hydrochloric acid (37%) were purchased from Merk, and aluminum foil and MB were purchased from Fluka. Xray diffraction (XRD) pattern was recorded with an Xray diffractometer (SHIMADZUXD-DL) using CuK_α radiation (λ = 1.5418 Å) at 35.4 kV and 28 mA with a scanning speed of 2θ = 10° min^{-1}. Fourier transform infrared (FTIR) spectrum was recorded with an FTIR spectrometer (Tensor 27Bruker) at room temperature in the range of 400–1300 cm^{-1}. Scanning electron microscopy (SEM; EM-3200, KYKY) was used to determine the crystallite size and morphology of the sample. Nitrogen adsorption-desorption isotherms were measured at 77 K using a Quantachrome NovaWin2 apparatus. For each set of experiments, the residual MB concentrations in the supernatant were analyzed using a T90+ -UV-vis spectrophotometer. The pH measurements were made with a pH meter, model 827 pH lab, Metrohm, Switzerland.

2. 2. Synthesis of Nanozeolite L

In order to synthesize nonozeolite L, silica and alumina solutions were prepared by dissolving 20 mmol silicic acid and 2 mmol aluminum foil in potassium hydroxide solutions, respectively. Then, the silica solution was added dropwise to the alumina solution under vigorous stirring. The resulting aluminosilicate gel was transferred into a Teflon-lined stainless steel autoclave and heated at 170°C for 2 days. The resulting product was then centrifuged, washed with deionized water, and dried at 80 °C.

2. 3. MB Sorption Experiments

Batch adsorption experiments were performed to investigate the adsorption behavior of MB onto synthesized nanozolite L in aqueous solution at 25°C. The effect of pH was studied in the range of 2-10 and the pH values were adjusted using 0.1 M HCl and 0.1 M NaOH solutions. To investigate the effect of pH, 5 mg of nanozeolite L was added to 10 mL of each MB solution (20 mg L^{-1}) and the solutions were shaken for 30 minutes.

To study the effect of adsorbent dosage, 10 mL of 20 mg L^{-1} MB solution at pH = 9 was shaken with 2–15 mg of nanozeolite L for 30 minutes.

To study the kinetics of the adsorption process, MB solution containing 0.5 g L^{-1} of nanozeolite L at pH = 9 was vigorously agitated for different times in the range of 5–40 minutes. For adsorption isotherm studies, constant dosages of nanozeolite L (0.5 g L^{-1}) were agitated with different initial concentrations of MB in the range of 20–100 mg L^{-1} at pH = 9.

Also, the temperature effect on adsorption was studied by mixing 5 mg of nanozeolite L with 10 mL of 40 mg L^{-1} MB solution at different temperatures ranged from 25 to 55 °C.

At the end of the experiments, samples were centrifuged and the residual concentrations of MB were determined using UV-Vis spectrophotometer. The removal percentage was determined from equation (1):

$$\text{Removal (\%)} = \frac{C_i - C_e}{C_i} \times 100 \quad (1)$$

where C_i and C_e (mg L^{-1}) are the concentrations of MB in initial solution and the aqueous phase after adsorption, respectively. Also, the adsorption capacity (q_e, mg g^{-1}) of nanozeolite L was calculated using the following equation:

$$q_e = \frac{(C_i - C_e)V}{m} \times 100 \quad (2)$$

where V (L) is the volume of the aqueous phase and m is the weight of adsorbent.

3. Results and Discussion

3. 1. Characterization of Nanozeolite L

Figure 1a shows the XRD pattern of nanozeolite L. The presence of the characteristic peaks of nanozeolite L at 2θ = 5.5°, 19.4°, 22.7°, 25.6°, 28.0°, 29.1°, and 30.7° in the diffraction pattern indicates that the pure phase of nanozeolite L is formed.[28] The FTIR spectrum (inset, Fig 1a) shows the characteristic vibrational bands of nanozeolite L in the range of 400–1300 cm^{-1}. The broadband in the range 1008–1145 cm^{-1} shows the asymmetric stretching vibrations of O–T–O (T=Si, Al) tetrahedral. The adsorption

band near 721 cm^{-1} belongs to the symmetric stretching vibrations of O–T–O, and the band near 765 cm^{-1} is related to the symmetric stretching vibrations of AlO_4 tetrahedral. The band around 605 cm^{-1} is attributed to the vibration of double six-membered rings (D6Rs), and the band near 476 cm^{-1} is assigned to the O–T–O bending vibrations.[29]

The size and surface morphology of synthesized nanozeolite L was revealed from its SEM image. The formation of spherical-like nanoparticles with an average diameter of about 20 nm could be observed in Figure 1b.

The elemental analysis of the synthesized nanozeolite L was investigated through EDX studies, and the results are represented in Figure 1c. As can be seen in the figure, the elemental content of synthesized nanozeolite consists of oxygen (O), aluminum (Al), silicon (Si), and potassium (K), with the weight percentages of 42.37, 27.48, 20.14, and 10.01.

The textural properties of nanozeolite sample were investigated by N_2 sorption analysis. The nitrogen adsorption-desorption isotherms of nanozeolite L prepared sample is shown in Fig 1d. It shows type IV isotherm with an H_1 type hysteresis loop which is found in well-defined cylindrical pores or material agglomerates consisting of extremely uniform particles.[30] The results showed that the specific surface area of the prepared sample is 215 $m^2\ g^{-1}$. Also, the pore volume of synthesized nanozeolite obtained 0.4 cc g^{-1}, and its pore size distribution is centered at about 3.65 nm (inset, Figure 1d).

3. 2. Adsorption Studies

3. 2. 1. Effect of pH

The initial pH plays an important role in the adsorption process. The effect of solution pH on MB removal by the synthesized nanozeolite was investigated in the range of 2–10. As shown in Figure 2, the adsorbed MB increased

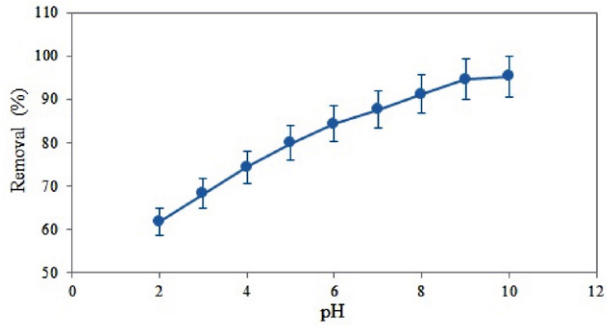

Figure 2. Effect of pH on MB adsorption by nanozeolite L

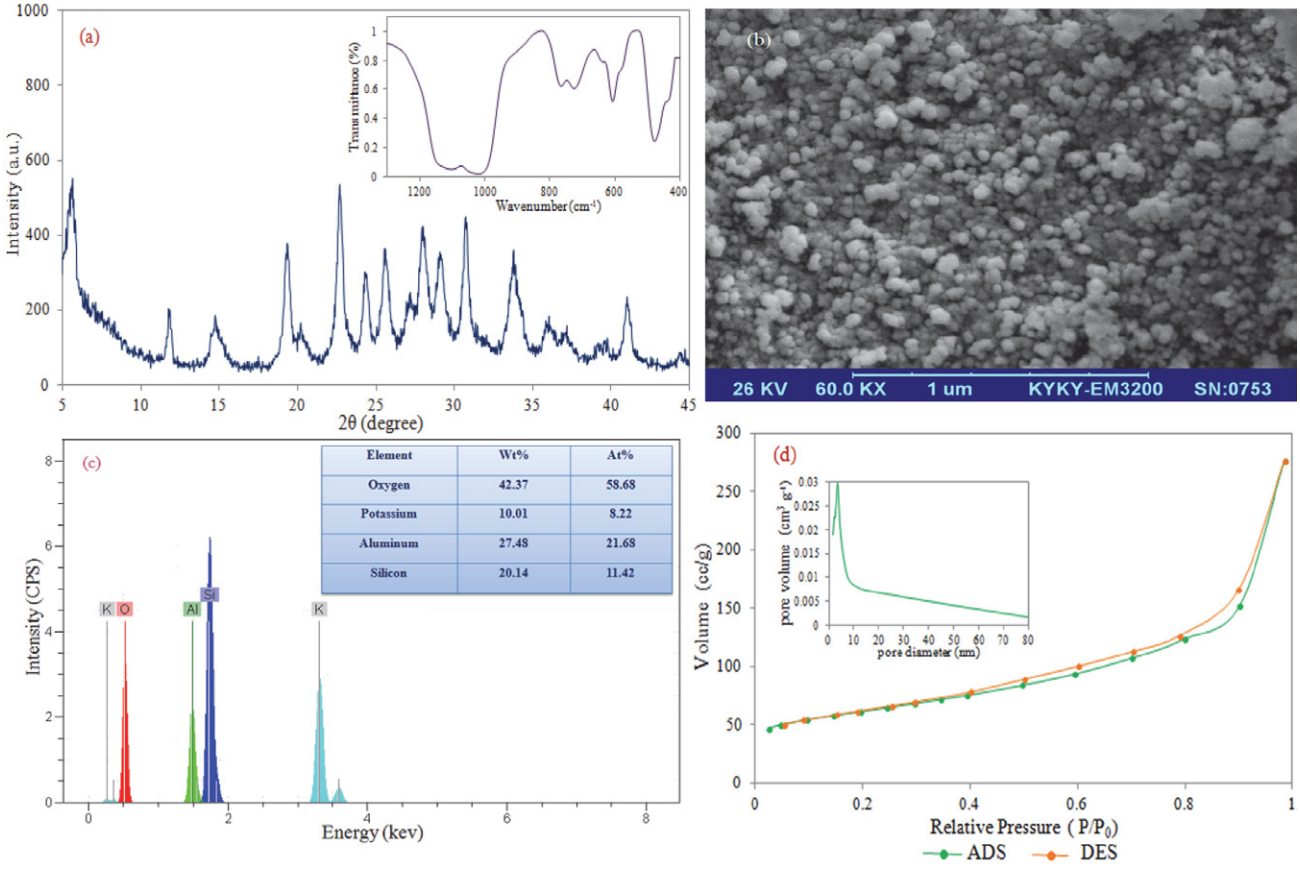

Element	Wt%	At%
Oxygen	42.37	58.68
Potassium	10.01	8.22
Aluminum	27.48	21.68
Silicon	20.14	11.42

Figure 1. (a) XRD pattern of synthesized nanozeolite L, Inset: FT-IR spectrum of nanozeolite L, (b) SEM image of nanoparticles of zeolite L, (c) EDX spectrum of nanozeolite L, (d) Nitrogen adsorption-desorption isotherms of nanozeolite L, Inset: pore size distribution of nanozeolite L

with increasing solution pH and reached its maximum at pH = 9. It is probably due to the presence of H^+ ions at lower pH, which will compete with cationic MB for adsorption sites. As pH increases, the zeolite surface is more negatively charged, which results in an increment of adsorption because of the decrease in the electrostatic repulsion force between MB and zeolite surface.[31,32]

3. 2. 2. Effect of Adsorbent Dosage

Adsorbent dosage is an important factor in the adsorption process because it defines the capacity of an adsorbent for a given initial concentration of the adsorbate. Figure 3 shows the effect of adsorbent dosage on the adsorption of MB. The figure shows that the optimum dosage of nanozeolite L for the removal of MB is 5 mg. The further increase in the amount of MB removal was found to be negligible above a dose of 5 mg. The increase in the extent of MB removal with the adsorbent dose is attributed to the increase in the adsorbent surface area and thus the number of adsorption sites available for adsorption.[33]

3. 2. 3. Effect of Contact Time and Kinetic Studies

Figure 4a shows the effect of contact time on the adsorption process of MB on synthesized nanozeolite sodalite. As can be observed in the figure, the dye removal efficiency was increased as the contact time increased until equilibrium.[34] The adsorption equilibrium with nanozeolite sodalite was reached at 30 min.

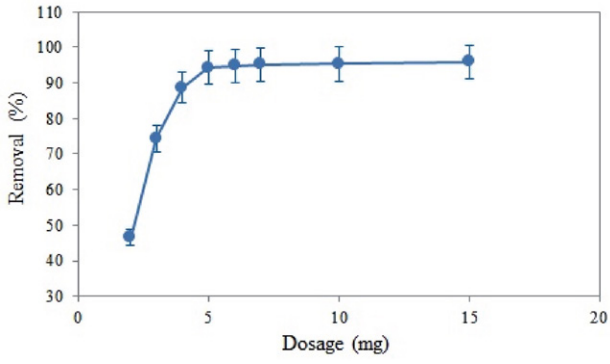

Figure 3. Effect of adsorbent dosage on MB adsorption by nanozeolite L

To evaluate the mechanism of adsorption, pseudo-first-order and pseudo-second-order models were investigated to find the best-fitted model for the experimental data. When the adsorption process is diffusion-controlled, the kinetics follows the pseudo-first-order model, and when the adsorption process occurs through the chemisorption mechanism, the adsorption kinetics follows the pseudo-second-order model. These models are expressed by the following equations:[35,36]

$$\log(q_e - q_t) = \log q_e - \frac{K_1}{2.303} t \quad (3)$$

$$\frac{t}{q_t} = \frac{1}{K_2 q_e^{\,2}} + \frac{1}{q_e} t \quad (4)$$

where q_e and q_t are the adsorption capacity (mg g^{-1}) of the adsorbent at the equilibrium and at time t, respectively. Also, K_1 (min^{-1}) and K_2 (g mg^{-1} min^{-1}) are the rate constants of the pseudo-first-order and the pseudo-second-order adsorption and can be obtained from the log (q_e–q_t) versus t plot (Figure 4b) and t/q_t versus t plot (Figure 4c), respectively.

The obtained kinetic parameters of the models and coefficients of determination (R^2) are presented in Table 1. From the R^2 values, it can be deduced that the pseudo-second-order model fits the experimental data slightly better than the pseudo-first-order model.

3. 2. 4. Effect of MB Concentration and Isotherms Studies

The effect of the initial concentration of MB on its removal percentage by nanozeolite L was investigated, and the results are presented in Figure 5a. The results show that as the initial dye concentration increases, the removal percentage decreases due to the consumption of the available active adsorption sites on the adsorbent.[37]

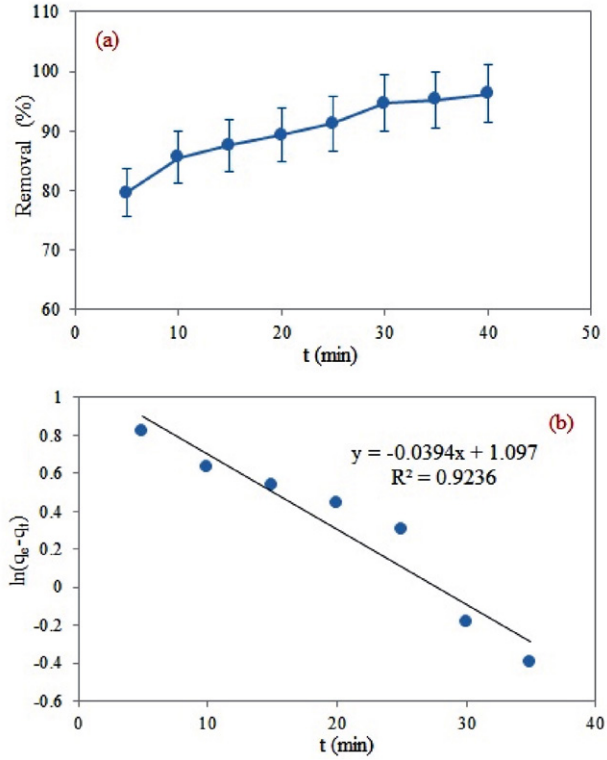

Figure 4. (a) Effect of contact time on MB adsorption by nanozeolite L, (b) Pseudo-first-order kinetics plots for adsorption of MB by nanozeolite L and (c) Pseudo-second-order kinetics plots for adsorption of MB by nanozeolite L

Table 1. Kinetic parameters of pseudo-first-order model and pseudo-second-order model for MB adsorption by nanozeolite L

Models	Parameters	values
pseudo-first-order	K_1 (min^{-1})	0.0907
	$q_{e,\,cal}$ (mg g^{-1})	12.50
	R^2	0.9236
pseudo-second-order	K_2 (g mg^{-1} min^{-1})	0.0140
	$q_{e,\,cal}$ (mg g^{-1})	39.84
	R^2	0.9989
Experimental data	$q_{e,exp}$ (mg g^{-1})	38.49

The adsorption isotherm studies are important for distinguishing the nature of adsorption. The adsorption isotherm experimental data were analyzed with Langmuir and Freundlich models.

Langmuir isotherm is used for the monolayer adsorption on a homogenous surface and is expressed as follows:[38]

$$\frac{C_e}{q_e} = \frac{1}{q_{max} K_L} + \frac{1}{q_{max}} C_e \quad (5)$$

where C_e is the dye concentration at the equilibrium (mg L^{-1}); q_e is the equilibrium adsorption capacity (mg g^{-1}); q_{max} is the maximum monolayer uptake capacity of the adsorbent and K_L is the Langmuir equilibrium constant (L mg^{-1}). q_{max} and K_L can be obtained from the plot of C_e/q_e versus C_e (Figure 5b).

Freundlich isotherm is used to describe the multilayer adsorption equilibrium on the heterogeneous surface and is mathematically described by the following equation:[39]

$$\ln q_e = \ln K_F + \left(\frac{1}{n}\right) \ln C_e \quad (6)$$

where K_F is the Freundlich constant related to adsorbent capacity, and n is the heterogeneity factor which indicates the adsorption intensity. The values of K_F and n can be obtained from ln q_e versus ln C_e plot (Figure 5c).

The Langmuir and Freundlich isotherm constants, along with the correlation coefficients, are presented in Table 2. As can be seen in the table, the obtained correlation coefficient value is better for Langmuir isotherm, and the equilibrium adsorption capacity ($q_{max,\,cal}$) obtained from the Langmuir model is close to the experimentally observed saturation capacity ($q_{max,exp}$). So, it could be concluded that the equilibrium data for MB adsorption onto nanozeolite L gave a better fit to the Langmuir model.

3. 2. 5. Comparison with Other Adsorbents

Among several adsorbents reported in the literature for the removal of MB from aqueous solutions, some of them are summarized in Table 3. It can be observed that the adsorption capability of nanozeolite L is greater than most of those reported for other adsorbents. This can be attributed to a higher amount of adsorption sites of nanozeolite L and confirms that it can be used as a promising sorbent for MB removal from its aqueous solution.

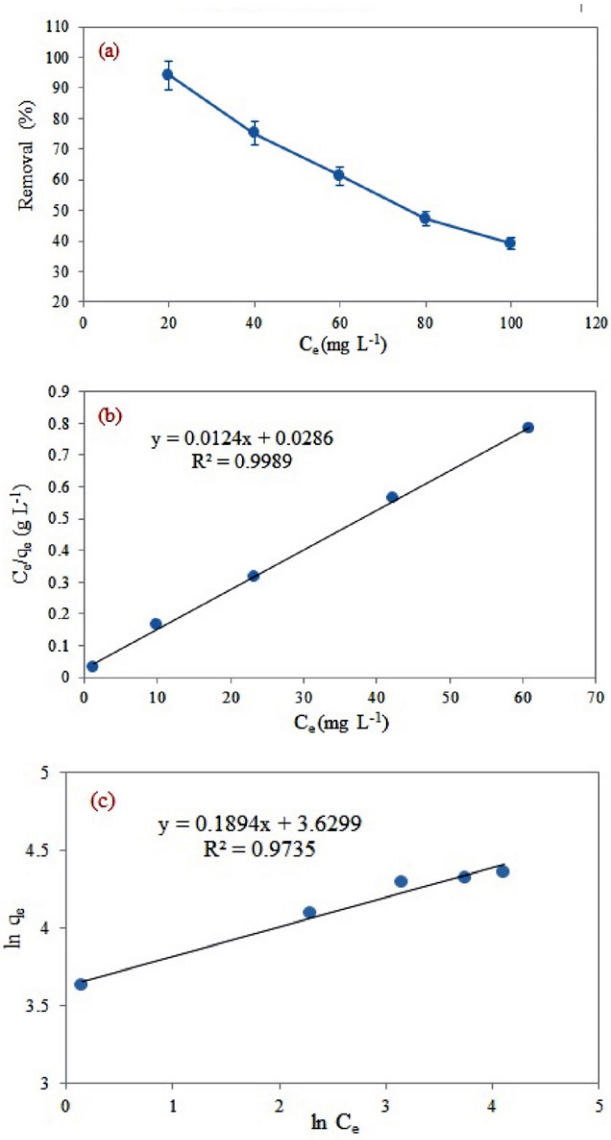

Figure 5. (a) Effect of initial concentration on MB adsorption by nanozeolite L, (b) Langmuir isotherm for MB adsorption by nanozeolite L and (c) zeolite Freundlich isotherm for MB adsorption by nanozeolite L

Table 2. Isotherm parameters for MB adsorption by nanozeolite L

Isotherm	Parameters	values
Langmuir	$q_{max,\,cal}$ (mg g^{-1})	80.64
	K_L (L mg^{-1})	0.43
	R^2	0.9989
Freundlich	K_F (mg g^{-1}(L mg^{-1}) $^{1/n}$)	37.71
	n_F (mg g^{-1})	5.28
	R^2	0.9735
Experimental data	$q_{max,exp}$ (mg g^{-1})	78.00

3. 2. 6. Effect of Temperature and Thermodynamic Studies

In this study, the effect of temperature on MB adsorption was investigated in the range of 298–328 K. The results (Figure 6) showed that the percentage removal increased with the increment of temperature. This can be attributed to the increase of dye molecule mobility with temperature.

As the reaction temperature in the solution increases, the number of molecules which have enough energy to undergo an interaction with active sites at the surface increases.[40,41]

Table 3. Comparison of maximum adsorption capacities of various adsorbents for MB

Adsorbent	q_m (mg g^{-1})	Reference
Kaolinite	45.60	[42]
Magnetic multi-wall carbon nanotube	15.87	[43]
Walnut shells	51.55	[44]
Freeze–dried agarose gel	10.40	[45]
Zeolite A	64.80	[46]
Cortaderia selloana flower spikes	47.90	[47]
ZSM-5	8.67	[48]
Algerian palygorskite powder	57.50	[49]
(Chit/AILP-Kao) nanocomposite	99.01	[50]
Fly ash based spheres	79.70	[51]
Sodium dodecyl benzenesulfonate modified ZSM-5	15.68	[48]
Rice husk	40.59	[52]
Zeolite/Ferrite Nickel/Alginate nanocomposite	54.05	[53]
Nanozeolite L	80.64	This work

The Increase of percentage removal with temperature demonstrates that the adsorption process is endothermic. Thermodynamic parameters (ΔG°, ΔH°; ΔS°) values were calculated using the following equations:

$$\Delta G^{\circ} = -R\,T\,\ln K_C \tag{7}$$

$$\ln K_C = \frac{\Delta S^{\circ}}{R} - \frac{\Delta H^{\circ}}{RT} \tag{8}$$

where R (8.314 J $mol^{-1}K^{-1}$) is the universal gas constant, T (K) is the absolute temperature, and K_c is the ratio of MB concentration adsorbed on the adsorbent at equilibrium and MB concentration remaining in solution at equilibrium. The values of ΔH° and ΔS° can be obtained from the slope and intercept of ln k_d versus 1/T plot, respectively. The obtained values of thermodynamic parameters are tabulated in Table 4. ΔG° values obtained negative, indicating that the adsorption process is thermodynamically feasible and spontaneous at room temperature.

The positive ΔS° value for MB adsorption onto nanozeolite L is due to increasing randomness at the solid-solution interface during the adsorption process.

The Values of ΔG° are negative, confirming that the adsorption process is thermodynamically feasible and spontaneous in nature. The obtained positive value of ΔH° reveals the endothermic nature of the adsorption process, and the calculated positive value of ΔS° is related to the increase of randomness at the solid-solution interface during the adsorption process.

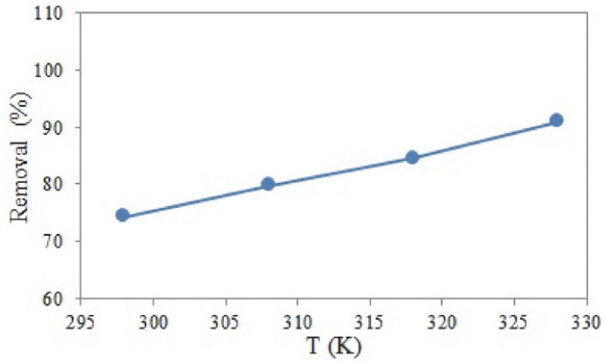

Figure 6. Effect of temperature on MB adsorption by nanozeolite L

Table 4. Thermodynamic parameters for MB adsorption by nanozeolite L

Temperature (K)	Kc	ΔG° (kJ mol^{-1})	ΔH° (kJ mol^{-1})	ΔS° (J K^{-1} mol^{-1})
298	2.880	–2.621	–26.256	96.66
308	3.998	–3.549		
318	5.446	–4.481		
328	7.690	–5.563		

4. Conclusion

Uniform nanoparticles of zeolite L were synthesized via a hydrothermal approach. Then the feasibility of using synthesized nanozeolite L as an adsorbent for MB removal was investigated.

The removal efficiency was optimized at a reaction time of 30 min at pH 9 and an adsorbent dose of o.5 g l^{-1}. The experimental adsorption isotherm data were best fitted with the Langmuir model with a maximum sorption capacity of 80.64 mg g^{-1}. The better R^2 showed that the kinetics of the system could be conveniently modeled by the pseudo-second-order model, indicating that the rate controlling step is a chemisorption mechanism. The thermodynamic studies represent that the adsorption process is endothermic, feasible, and spontaneous in nature.

Based on these evidences, nanozeolite L with high adsorption capacity and low preparation cost can be used as an efficient and cost-effective adsorbent for the removal of MB from wastewater. For example, using this zeolite to separate MB from wastewater of dye and textile factories

can be applicative; also the ability of this zeolite can be examined to separate other industrial dyes wastewater.

5. References

1. V. K. Gupta, A. Mittal, L. Krishnan, J. Mittal, *J. Colloid. Interf. Sci.* **2006**, *293*, 16–26. **DOI:**10.1016/j.jcis.2005.06.021
2. R. Han, Y. Wang, W. Zou, Y. Wang, J Shi, *J. Hazard. Mater.* **2007**, *145*, 331–335. **DOI:**10.1016/j.jhazmat.2006.12.027
3. E. N. El-Qada, S. J. Allen, G. M. Walker, *Chem. Eng. J.* **2006**, *124*, 103–110. **DOI:**10.1016/j.cej.2006.08.015
4. M. Ghaedi, S. Heidarpour, S. Nasiri Kokhdan, R. Sahraie, A. Daneshfar, B. Brazesh, *Powder Technol.* **2012**, *228*, 18–25. **DOI:**10.1016/j.powtec.2012.04.030
5. K. Mahapatra, D. S. Ramteke, L. J. Paliwal, *J. Anal. Appl. Pyrol.* **2012**, *95*, 79–86. **DOI:**10.1016/j.jaap.2012.01.009
6. J. Z. Yi, L. M. Zhang, *Bioresour. Technol.* **2008**, *99*, 2182–2186. **DOI:**10.1016/j.biortech.2007.05.028
7. N. Salek Gilani, S. Ehsani Tilami, S. N. Azizi, *J. Chin. Chem. Soc.* **2021**, *68*, 2264–2273. **DOI:**10.1002/jccs.202100258
8. A. E. Ofomaja, *Chem. Eng. J.* **2008**, *143*, 85–95. **DOI:**10.1016/j.cej.2007.12.019
9. V. K. Garg, R. Gupta, A. Bala Yadav, R. Kumar, *Bioresour. Technol.* **2003**, *89*, 121–124. **DOI:**10.1016/S0960-8524(03)00058-0
10. A. R. Tehrani-Bagha, H. Nikkar, N. M. Mahmoodi, M. Markazi, F. M. Menger, *Desalination* **2011**, *266*, 274–280. **DOI:**10.1016/j.desal.2010.08.036
11. B. H. Hameed, A. L. Ahmad, and K. N. A., Latiff, *Dyes Pigm.* **2007**, *75*, 143–149. **DOI:**10.1016/j.dyepig.2006.05.039
12. S. M. Sidik, A.A.Jalil, S. Triwahyono, S. H. Adam, M. A. H. Satar, B. H. Hameed, *Chem. Eng. J.* **2012**, *203*, 9–18. **DOI:**10.1016/j.cej.2012.06.132
13. A. A. Jalil, S. Triwahyono, M. R. Yaakob, Z. Z. A. Azmi, N. Sapawe, N. H. N. Kamarudin, H. D. Setiabudi, N. F. Jaafar, S. M. Sidik, S. H. Adam, B. H. Hameed, *Bioresour. Technol.* **2012**, *120*, 218–224. **DOI:**10.1016/j.biortech.2012.06.066
14. E. Bulut, M. Ozacar, I. A. Sengil, *J. Hazard. Mater.* **2008**, *154*, 613–622. **DOI:**10.1016/j.jhazmat.2007.10.071
15. C. C. Wang, L. C. Juang, T. C. Hsu, C. K. Lee, F. C. Huang, *J. Colloid Interface Sci.* **2004**, *273*, 80–86. **DOI:**10.1016/j.jcis.2003.12.028
16. M. H. Karaoglu, M. Dogan, M. Alkan, *Micropor. Mesopor. Mat.* **2009**, *122*, 20–27.
17. R. Han, Y. Wang, Q. Sun, L. Wang, J. Song, X. He, C. Dou, *J. Hazard. Mater.* **2010**, *175*, 1056–1061. **DOI:**10.1016/j.jhazmat.2009.10.118
18. S. J. Allen, E. Ivanova, B Koumanova, *Chem. Eng. J.* **2009**, *152*, 389–395. **DOI:**10.1016/j.cej.2009.04.063
19. B. A. Shah, A. V. Shah, R. V. Tailor, *J. Disper. Sci. Technol.* **2012**, *33*, 41–51. **DOI:**10.1080/01932691.2010.530079
20. B. A. Shah, C. B. Mistry, A. V. Shah, *Chem. Eng. J.* **2013**, *220*, 172–184. **DOI:**10.1016/j.cej.2013.01.056
21. A. S. Ozcan, B. Erdem, A. Ozcan, *Colloid Surface A* **2005**, *266*, 73–81.
22. S. N. Azizi, S. Ghasemi S, and N. Salek Gilani, *Chinese J. Catal.* **2014**, *35*, 383-390. **DOI:**10.1016/S1872-2067(14)60002-4
23. A. Mech, A. Monguzzi, F. Meinardi, J. Mezyk, G. Macchi, R. Tubino, *J. Am. Chem. Soc.* **2010**, *132*, 4574–4576. **DOI:**10.1021/ja907927s
24. S. N. Azizi, S. Ghasemi S, N. Salek Gilani, *Monatsh. Chem.* **2016**, *147*, 1467–1474. **DOI:**10.1007/s00706-016-1664-3
25. M. J. Climent, A. Corma, S. Iborra, *Chem. Rev.* **2011**, *111*, 1072-1133. **DOI:**10.1021/cr1002084
26. L. Tosheva L, V. P. Valtchev, *Chem. Mater.* **2005**, *17*, 2494–2513. **DOI:**10.1021/cm047908z
27. N. Salek Gilani, S. N. Azizi, S. Ghasemi, *Bull. Mater. Sci.* **2017**, *40*, 177–185. **DOI:**10.1007/s12034-016-1351-3
28. L. J. Garces, V. D. Makwana, B. Hincapie, A. Sacco, S.L. Suib, *J. Catal.* **2003**, *217*, 107–116.
29. Y.S. Ko, W.S. Ahn, *Bull. Korean Chem. Soc.* **1999**, *20*, 1–6.
30. M. Thommes, **2010**, *82*, 1059–1073. **DOI:**10.1002/cite.201000064
31. G. Zhang, Y. Bao, *Energy Proc.* **2011**, *16*, 1141–1146. **DOI:**10.1016/j.egypro.2012.01.182
32. P. K. Mondal, R. Ahmad, R. Kumar, *Environ. Eng. Manag. J.* **2014**, *13*, 231–240. **DOI:**10.30638/eemj.2014.026
33. R. Ahmad, *J. Hazard. Mater.* **2009**, *171*, 767–773. **DOI:**10.1016/j.jhazmat.2009.06.060
34. T. C. R. Bertolini, J. C. Izidoro, C. P. Magdalena, D. A. Fungaro, *Orbital: Electron J. Chem.* **2013**, *5*, 179–191.
35. Y. S. HO, G. McKay, *Can. J. Chem. Eng.* **1998**, *76*, 822–826. **DOI:**10.1002/cjce.5450760419
36. Y. S. Ho, D. J. Wase, C. F. Forster, *Technol.* **1996**, *17*, 71–77. **DOI:**10.1080/09593331708616362
37. S. A. Drweesh, N. A. Fathy, M. A. Wahba, A. A. Hanna, A. I. Akarish, E. A. Elzahany, K. S. *J. Environ. Chem. Eng.* **2016**, *4*, 1674–1684. **DOI:**10.1016/j.jece.2016.02.005
38. I. Langmuir, *J. Am. Chem. Soc.* **1918**, *40*, 1361–1403. **DOI:**10.1021/ja02242a004
39. H. M. F. Freundlich, *J. Phys. Chem.* **1906**, *57*, 385–470. **DOI:**10.1515/zpch-1907-5723
40. S. Netpradit, P. Thiravetyan, S. Towprayoon, *J. Colloid Interface Sci.* **2004**, *270*, 255–261. **DOI:**10.1016/j.jcis.2003.08.073
41. F. Birch, *J. Geophys. Res.* **1986**, *91*, 4949–4954. **DOI:**10.1029/JB091iB05p04949
42. S. Asuha, F. Fei, W. Wurendaodi, S. Zhao, H. Wu, and X. Zhuang, *Powder Technol.* **2019**, *361*, 624–632. **DOI:**10.1016/j.powtec.2019.11.068
43. J. L. Gong, B Wang, G. M. Zeng, C. P. Yang, C. G. Niu, Q. Y. Niu, W. J. Zhou, Y. Liang, *J. Hazard. Mater.***2009**, *164*, 1517–1522. **DOI:**10.1016/j.jhazmat.2008.09.072
44. R. Tang, C. Dai, C. Li, W. Liu, S. Gao, C. Wang, *J. Chem.* **2017**, *2017*, 1–10. **DOI:**10.1155/2017/8404965
45. W. Y. Seow, C. A. E. Hauser, *J. Environ. Chem. Eng.* **2016**, *4*, 1714–1721. **DOI:**10.1016/j.jece.2016.02.013
46. N. Sapawe, A. A. Jalil, S. Triwahyono, M. I. A. Shah, R. Jusoh, N. F. M. Salleh, A. H. Karim, *Chem. Eng. J.* **2013**, *229*, 388-398. **DOI:**10.1016/j.cej.2013.06.005

47. N. Mechi, I. B. Khemis, G. L. Dotto, D. Franco, L. Sellaoui, A. B. Lamine, *J. Mol. Liq.* **2019**, *280*, 268–273. **DOI:**10.1016/j.molliq.2019.02.024
48. X. Jin, M. Jiang, X. Shan, Z. Pei, Z. Chen, *J. Colloid Interface Sci.* **2008**, *328*, 243–247. **DOI:**10.1016/j.jcis.2008.08.066
49. L. D. Youcef, L. S. Belaroui, A. L. Galindo, *Appl. Clay Sci.* **2019**, *179*, 105145. **DOI:**10.1016/j.clay.2019.105145
50. R. Ahmad, K. Ansari, Process Biochem. 2021, *108*, 90–102. **DOI:**10.1016/j.procbio.2021.05.013
51. R. M. Novais, J. Carvalheiras, D. M. Tobaldi, M. P. Seabra, R. C. Pullar, J. A. Labrincha, *J. Clean. Prod.* **2019**, *207* 350–362. **DOI:**10.1016/j.jclepro.2018.09.265
52. V. Vadivelan, K. V. Kumar, *J. Colloid Interface Sci.* **2005**, *286*, 90–100. **DOI:**10.1016/j.jcis.2005.01.007
53. M. Bayat, V. Javanbakht, J. Esmaili, *Int. J. Biol. Macromol.* **2018**, *116*, 607–619. **DOI:**10.1016/j.ijbiomac.2018.05.012

Povzetek

Nanozeolit L je bil uporabljen kot adsorbent z namenom določitve njegove učinkovitosti za odstranjevanje strupenega barvila metilen modro (MB). Sintetizirani nanozeolit L je bil okarakteriziran z rentgensko difrakcijo (XRD), infrardečo Fourierjevo transformacijo (FTIR), elektronsko mikroskopijo (SEM), Brunauer-Emmett-Teller analizo (BET) in energijsko-disperzivno rentgensko spektroskopijo (EDX) za določitev njegovih osnovnih fizikalno-kemijske lastnosti. Adsorpcija je bila preučevana v odvisnosti od pH, količine adsorbenta, kontaktnega časa, začetne koncentracije MB in temperature. Adsorpcijsko obnašanje MB je bilo bolje opisano z Langmuirovo izotermo kot s Freundlichovo, največja adsorpcijska zmogljivost nanozeolita L pa je bila dosežena pri 80,64 mg g^{-1}. Negativna vrednost Gibbsove proste energije ($\Delta G°$) in pozitivna vrednost standardne spremembe entalpije ($\Delta H°$) sta potrdili, da je proces adsorpcije spontan in endotermen. Na podlagi teh ugotovitev je nanozeolit L z veliko površino, veliko adsorpcijsko zmogljivostjo in nizkimi stroški sinteze lahko učinkovit in ekonomičen adsorbent za odstranjevanje MB.